

pubs.acs.org/Biomac Article

Stabilization of Synthetic Collagen Triple Helices: Charge Pairs and Covalent Capture

Published as part of the Biomacromolecules virtual special issue "Peptide Materials".

Carson C. Cole, Le Tracy Yu, Mikita Misiura, Joseph Williams, III, Thi H. Bui, and Jeffrey D. Hartgerink*



Cite This: Biomacromolecules 2023, 24, 5083-5090



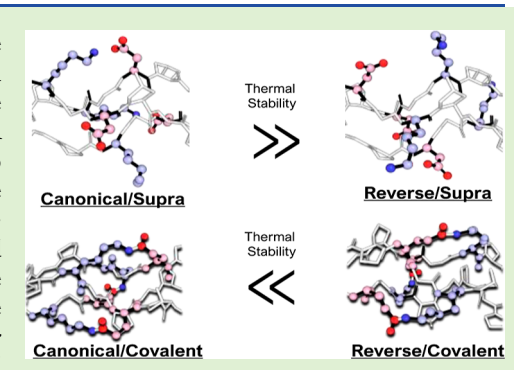
ACCESS

III Metrics & More

Article Recommendations

Supporting Information

ABSTRACT: Collagen mimetic peptides are composed of triple helices. Triple helical formation frequently utilizes charge pair interactions to direct protein assembly. The design of synthetic triple helices is challenging due to the large number of competing species and the overall fragile nature of collagen mimetics. A successfully designed triple helix incorporates both positive and negative criteria to achieve maximum specificity of the supramolecular assembly. Intrahelical charge pair interactions, particularly those involved in lysine—aspartate and lysine—glutamate pairs, have been especially successful both in driving helix specificity and for subsequent stabilization by covalent capture. Despite this progress, the important sequential and geometric relationships of charged residues in a triple helical context have not been fully explored for either supramolecular assembly or covalent capture stabilization. In this study, we compare the eight canonical axial



and lateral charge pairs of lysine and arginine with glutamate and aspartate to their noncanonical, reversed charge pairs. These findings are put into the context of collagen triple helical design and synthesis.

■ INTRODUCTION

The stabilization of a higher-order assembly can be accomplished by using charge pair interactions. Charge pairs form between a cationic side chain, such as an amine or guanidinium group, and an anionic side chain, such as a carboxylate group. In globular proteins, the hydrophobic collapse varies the geometry and solvent exposure of a protein depending on the extent of folding. In the unfolded state, there is typically a higher net charge for the protein, and upon folding, a decrease is observed. Charge pair interactions are important for other protein types, such as transmembrane, protein—protein, and hydrophilic assemblies. Additionally, collagen's tertiary structure, known as the triple helix, is stabilized by charge pair interactions.

Collagen triple helical assemblies are challenging targets for synthesis. The repetitious nature of the primary sequence, (Xaa–Yaa–Gly),, where frequently Xaa is proline (P) and Yaa is hydroxyproline (O), belies many of the challenges of directing assembly.^{3–5} Collagen assembly is frustrated by a large number of competing species near in energy, slow folding kinetics, and overall low thermal stability.^{6–8} Synthetic strategies have been employed in an attempt to overcome each of these issues.^{9–12}

Design criteria to select the correct assembly of collagen can be divided into the single amino acid propensity to stabilize a helix and pairwise amino acid interactions. Of the pairwise interactions, charge pairs between the cationic amino acids lysine (K) and arginine (R) and the anionic aspartate (D) and glutamate (E) have been studied in the greatest detail. By utilizing these charge pairs, control of assembly of biomimetic collagen heterotrimers has been achieved. ^{13–16} It has been found that in a triple helix, the pairwise charge pairs are presented in two distinct geometries, axial and lateral. ^{14,17–19} For example, a lysine—aspartate interaction in the axial geometry results in a large thermal stabilization, but a lateral geometry confirms little to no stabilization.

These interactions are also sequentially dependent. In natural collagens, cationic amino acids are frequently expressed in the Yaa position while anionic amino acids are usually in the Xaa position. Because of this propensity, most synthetic studies have retained this preference. The above-mentioned K–D pairs are rendered in Figure 1A and are termed "canonical axial charge pairs."

However, some studies have reversed this preference to generate noncanonical D-K axial and noncanonical D-K

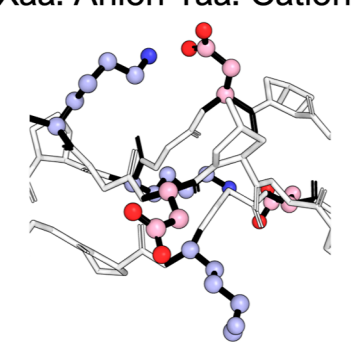
Received: July 10, 2023 Revised: October 9, 2023 Accepted: October 10, 2023 Published: October 23, 2023





a) Canonical (KGDO) Xaa: Anion Yaa: Cation

b) Reverse (DGKO) Xaa: Cation Yaa: Anion



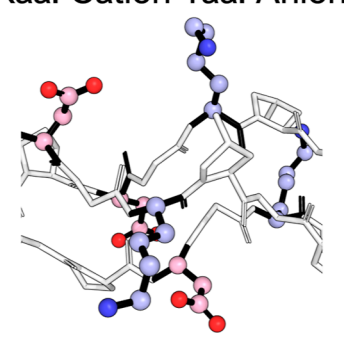


Figure 1. Energy-minimized canonical and reverse charge pairs in a triple helix. (a) KGDO interactions allow optimal salt bridge formation in triple helices and (b) switching the sequential positions of the anion and cation impacts the distance of interaction in salt bridges.

lateral charge pairs (see Figure 1b). 16,22,23 Here we call these noncanonical charge pairs "reverse" charge pairs to indicate the swapped position of the positive and negative amino acids.

There has yet to be a study performing a comprehensive analysis of the stabilizing propensity for the canonical and noncanonical charge pairs with explicit contributions from the pairwise interactions. Here, we perform studies on the eight noncanonical charge pairs and compare them to the eight canonical pairs. Of these eight noncanonical or reverse charge pairs, we find that two of them result in the stabilization of the triple helix. Additionally, the stabilizing geometry flips to favor lateral interactions in the noncanonical amino acid set. These results help define the design space for supramolecular triple helices.

Recently, our lab has used the formation of isopeptide bonds in a covalent capture strategy to increase the thermal stability of triple helices and expand their application scope. We extend this approach here by investigating the stabilization of noncanonical charge pairs by isopeptide amide bond formation. Covalent capture was successful, and interestingly, the overall stability for a covalently captured reverse charge imparts more stability than its canonical counterpart.

■ EXPERIMENTAL SECTION

Peptide Synthesis. For OGXY substituted peptides, a basis (POG)₈ peptide had the 13th and 14th amino acid residues substituted. The YGXO peptides had the 11th and 13th residues substituted with each charge pair component to form a pairwise interaction. Peptides were synthesized using standard Fmoc-protected amino acids on a low-loading rink amide MBHA (4-methylbenzhydrylamine) resin to leave final peptides with C-terminal amidation. 25% (v/v) piperidine in dimethylformamide (DMF) was used for deprotection. Coupling steps were done with HATU (hexafluorophosphate azabenzotriazole tetramethyl uronium) and diisopropylethylamine (DiEA) in DMF at a 1:4:4:6 equiv of resin/amino acids/ HATU/DiEA. The N-terminus was acetylated with a double addition of excess acetic anhydride and DiEA in dichloromethane (DCM). Peptides were cleaved from the resin with 7.5% v/v scavengers in trifluoroacetic acid (TFA). Scavengers used include triisopropylsilane, H₂O, and anisole. The TFA mixture was moved to a round-bottomed vessel and was removed by evaporation under nitrogen pressure. Cold diethyl ether precipitated the peptide from the remaining mixture of scavengers. This was centrifuged, and the ether was decanted and then repeated. Peptides were dissolved in H2O and filtered. They were then purified by reverse phase high-performance liquid chromatography (HPLC) with water and acetonitrile at a gradient of 0.7%/min on a 19 × 250 mm C-18 column. The water and acetonitrile were

both treated with 0.05% TFA. Samples were rotovapped, frozen, and lyophilized. Matrix-assisted laser desorption/ionization mass spectrometry (MALDI-MS) confirmed the correct peptide mass. Pure, lyophilized peptides were dissolved in 10 mM phosphate buffer to a working concentration of 3 mM. All concentrations were determined by mass.

Covalent Capture. Hydroxybenzotriazole (12 mM, HOBt) and 1-ethyl-3-[3-(dimethylamino)propyl]carbodiimide (120 mM EDC) solutions were prepared in 100 mM MES buffer pH 6.1. The 3 mM peptide solutions (in 100 mM MES buffer, pH 6.1, as previously described) were mixed with the EDC and HOBt solutions in equal volume to be a 1:40:4 ratio (isopeptide bond/EDC/HOBt) in the MES buffer. Thus, the final reaction mixture contained 1 mM peptide (1 mM isopeptide bonds), 40 mM EDC, and 4 mM HOBt in 100 mM MES. The reaction mixture was mixed well by vortexing and incubated at 5 °C. For the first 2 h, the solutions were mixed by vortexing every half hour to ensure homogeneity. For preparing and purifying the covalently captured peptides, additional activating agents (of the same concentration and volume) were added on day 4 to increase the yield of the trimer product. The reaction was quenched by addition of 1 M hydroxylamine in a 1:1 ratio v/v (reaction mixture/hydroxylamine), vortexed, and left to react at 25 °C. Equal volumes of 1 M HCl (as hydroxylamine) were added to neutralize pH prior to characterization or purification.

Circular Dichroism. The circular dichroism (CD) data were collected on a Jasco J-810 spectropolarimeter equipped with a Peltier temperature controller. Spectrum measurement was taken at 5 °C. The spectra scanning used a 1 mm cuvette and a peptide concentration of 0.3 and 1 mM phosphate buffer. The melting curves were collected from 5 to 85 °C with a heating rate of 10 °C/h at the wavelength (around 225 nm) that gives the maximum molar residue ellipticity (MRE) value of each sample. For the refolding experiment, the sample solution was kept at 85 °C for 30 min and the temperature was cooled down from 85 to 5 $^{\circ}$ C with a cooling rate of 10 $^{\circ}$ C/h. The melting and refolding data were collected using a 1 mm cuvette with a peptide concentration of 0.3 mM to obtain a better signal. The firstorder derivatives of the melting curves were calculated with the Savitzky-Golay smoothing algorithm, and the temperature at which the minimum derivative value appears was defined as the melting temperature. The MRE value was calculated with the equation, MRE = $(\theta \times m)/(c \times l \times nr \times 10)$ where θ represents the experimental ellipticity in millidegrees, m is the molecular weight of the peptide (g/ mol), c is the peptide concentration (mg/mL), l is the path length of the cuvette (cm), and nr is the number of amino acid residues in the

Molecular Dynamics. All-atom molecular dynamics (MD) simulations were utilized to understand side-chain interaction effects on the stability of the OGXY' and YGXO peptides. The initial structure of the homotrimer collagen was obtained from the crystal structure of (GPO)₉ with Protein Data Bank (PDB) id: 3BOS.²⁷ We

then focused our analysis around the central portion of the triple helix and applied the mutations of interest to each structure. Each homotrimer was solvated in a cubic box's center and with TIP3P water molecules in Gromacs. The resulting systems comprised roughly 167,000 atoms in a cubic box with sides of 12 nm. GROMACS 5.1 was used to carry out MD simulations using the AMBER14-ffSB force field. ^{28,29} According to the experimental conditions, pressure and temperature were kept at 1 bar and 300 K using Langevin dynamics in the NPT ensemble. Periodic boundary conditions were applied in all directions, and the particle mesh Ewald (PME) method was utilized to evaluate the electrostatic potentials.²⁸ First, energy minimization was run for 5000 steps. After that, 10 ns runs using first NVT and then NPT ensemble were performed to equilibrate the system. Lastly, 100 ns production runs were performed. A time step of 2 fs was chosen in all simulations, and snapshots of the systems were saved every 20 ps. The inter-residue distance was measured with the center of mass for the cation at the N ζ of lysine and C η for arginine. The anions' centers of mass were the $C\gamma$ and $C\delta$ for aspartate and glutamate, respectively.

Molecular Packing. DLPacker, a deep neural network (DNN) side-chain conformer predicting software, was used to predict anionic and cationic amino acids' interaction distances.³⁰ To build YGXO peptides, we replaced the 12th and 14th residues of the (GPO)₉ (PDB: 3B0S) structure with cations or anions; OGXY' homotrimer structures were constructed by substituting the 14th and 15th residues. Interaction distances were then measured with Schrodinger PyMol.³¹

RESULTS AND DISCUSSION

Supramolecular Stabilization by Reverse Charge Pairs. To find the relative interaction strength of each canonical and noncanonical pairwise interaction, we began with the single and double substitutions of the central triplets of a base peptide, (POG)₈. This was carried out for the cations, lysine and arginine, and the anions, aspartate and glutamate. All synthesized peptides are given in Table 1. From a single amino acid substitution, the propensity for an amino acid to

Table 1. Melting Temperatures of Salt-Bridge-Containing Collagen Mimetic Peptides (CMPs)

1	m (0.0)	1	m (0.0)			
sequence substitutions	$T_{\rm m}$ (°C)	sequence substitutions	$T_{\rm m}$ (°C)			
Basis Ac-(POG) ₃ POGPOG(POG) ₃ -NH ₂ ^a						
$OGPO^b$	50.0					
Xaa Ac-(POG) ₃ POGXOG(POG) ₃ -NH ₂						
$OGDO^b$	41.5	OGKO	43.5			
OGEO ^b	44.5	OGRO	42.5			
Yaa Ac-(POG) ₃ PYGPOG(POG) ₃ -NH ₂						
$KGPO^b$	40.5	DGPO	34.5			
$RGPO^b$	47.0	EGPO	41.4			
canonical reverse s			ge			
YGXO Ac-(POG) ₃ PYGXOG(POG) ₃ -NH ₂						
KGDO ^b	47.0	DGKO	32.5			
$RGDO^b$	42.0	DGRO	30.5			
KGEO ^b	43.5	EGKO	35.0			
$RGEO^b$	42.5	EGRO	35.0			
OGXY' Ac-(POG) ₃ POGXY'G(POG) ₃ -NH ₂						
OGDK ^b	32.0	OGKD	37.5			
$OGDR^b$	38.0	OGRD	37.0			
OGEK ^b	37.0	OGKE	36.0			
OGER ^b	42.5	OGRE	35.0			

^aThe underlined central portion of this basis peptide is substituted at the 13th and 14th positions for OGXY and the 11th and 13th positions for YGXO peptides. ${}^bT_{\rm m}$ values from ref 15.

destabilize the triple helix is determined by CD melting analysis (see Figure 2). For example, each arginine (R) in the Xaa position destabilizes the triple helix by 2.5 $^{\circ}$ C, but in the Yaa position, it destabilizes by only 1.0 $^{\circ}$ C. The propensity is then found by dividing the net destabilization by three, as shown in eqs 1 and 2.

When considering the effect of a pairwise interaction on triple helix stability, we compare the single substitution propensity to doubly substituted peptides, OGXY and YGXO. From previous studies, we know that in an OGXY substitution scheme, there are two lateral interactions that can occur, and in a YGXO substitution, two axial and one lateral interactions can form.²¹

$$Xaa_{\text{propensity}} = \frac{T_{\text{m}_{(POG)_8}} - T_{\text{m}_{OGXO}}}{3} \tag{1}$$

$$Yaa_{\text{propensity}} = \frac{T_{\text{m}_{(POG)_8}} - T_{\text{m}_{OGPY}}}{3}$$
 (2)

Equation 3 correlates the melting temperature of an OGXY to substitution with the unknown deconvoluted $YX_{lateral}$ interaction. Rearrangement into eq 4 finalizes the lateral deconvolution. The melting temperature of the YGXO substitution $T_{m_{YGXO}}$ can then be used to find the axial interaction (YX_{axial}) by rearrangement of eqs 5 to 6.

$$T_{\rm m_{OGXY}} = T_{\rm m_{(POG)_8}} - \Delta T_{\rm m_{OGXO}} - \Delta T_{\rm m_{OGPY}} + 2YX_{\rm lateral}$$
(3)

$${\rm YX_{lateral}} = \frac{T_{\rm m_{OGXY}} - T_{\rm m_{(POG)_8}} + \Delta T_{\rm m_{OGXO}} + \Delta T_{\rm m_{OGPY}}}{2} \tag{4}$$

$$T_{\rm m_{YGXO}} = T_{\rm m_{(POG)_8}} - \Delta T_{\rm m_{OGXO}} - \Delta T_{\rm m_{OGPY}} + {\rm YX_{lateral}}$$
$$+ 2{\rm YX_{axial}} \tag{5}$$

$$= \frac{T_{\text{m}_{\text{YGXO}}} - T_{\text{m}_{\text{(POG)}_8}} + \Delta T_{\text{m}_{\text{OGXO}}} + \Delta T_{\text{m}_{\text{OGPY}}} - YX_{\text{lateral}}}{2}$$
(6)

CD of all reverse salt-bridge-containing peptides shows a strong transition temperature for each disubstituted system, as shown in Figure 2. The deconvolution analysis of the reverse charge pairs reveals striking differences as compared to their canonical counterparts. In Table 2, the canonical charge pairs substantially stabilize for the K-D (7.3 °C) and the K-E (4.0 °C) axial interactions. All other canonical pairs are moderately stabilizing or destabilizing. Reverse charge pairs demonstrate significant stabilization only for the D-K (4.8 °C) and D-R (5.0 °C) lateral interactions, while all others are minimally stabilizing or destabilizing. While both of these reverse charge pair interactions initially appear to be well-suited for helix design, the poor overall stability of the peptide OGRD, due to the destabilizing propensity of the individual amino acids, suggests that the reverse lateral D-R charge pair will not be as useful as D-K.

Interaction Distance Determination with MD. The conformer of an amino acid residue largely determines the distance between pairwise interactions. Therefore, the prediction of charge pair side chains, or "packing," was carried out by using a DNN-based model called DLpacker. ³⁰ By using the steric packing in Figure 3, we found the distance between

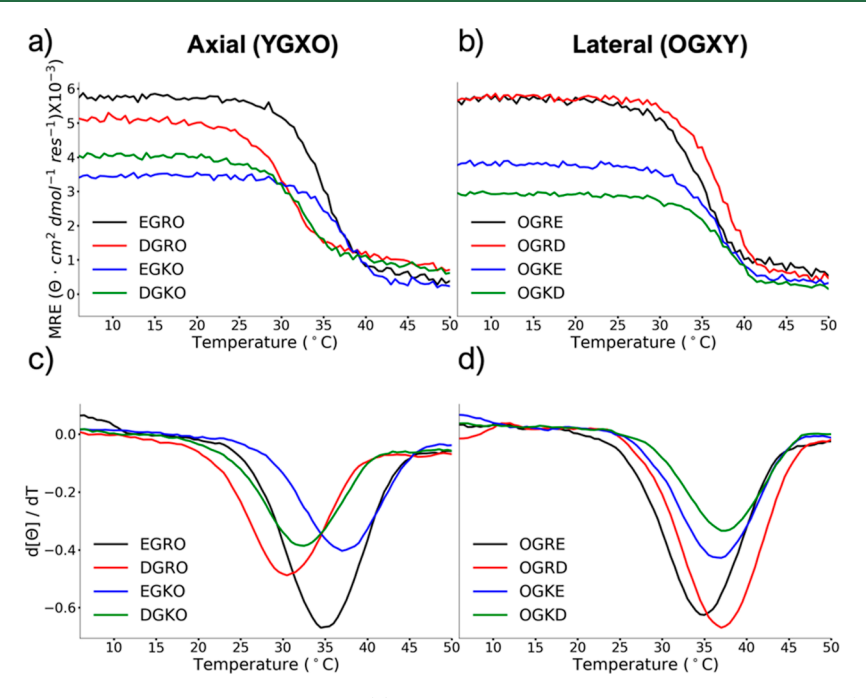


Figure 2. Thermal melts of reverse charge pairing triple helices. (a) YGXO-substituted CD thermal melting curves, (b) OGXY-substituted melt curves for reverse charge pairs, (c) YGXO-substituted CD thermal melt derivatives, and (d) OGXY-substituted melt derivatives.

Table 2. Deconvoluted Pairwise Interactions for Canonical and Reverse Charge Pairs^c

canonical	$Ax.^a$ (°C)	$Lat.^{b}$ (°C)	reverse	$Ax.^a$ (°C)	$Lat.^{b}$ (°C)
KD	7.3	-0.5	DK	-0.2	4.8
KE	4.0	1.0	EK	1.1	0.5
RD	1.3	-1.5	DR	-0.8	5.0
RE	-0.1	-0.3	ER	0.3	0.8

"The deconvolution of an axial charge pair (YX_{axial}) from eq 6. "The deconvolution of a lateral charge pair (YX_{lateral}) from eq 4. "Bolded pairwise interactions denote stabilizing charge pairs."

the canonical and reverse salt bridges to vary greatly. Effective salt bridges must be within 5 Å.³² However, the symmetry of the triple helix determines the proximity of the amino acid residues.²³ In Figure 3a, the disparity of distance KGDO and DGKO of 2.7 and 6.8 Å is significant.³³ Likewise, a stabilizing lateral interaction in OGRD is 4.3 Å, and for the destabilizing OGDR, the lateral interaction is 6.7 Å (see Figure 3b).

We simulated and compared the interaction distance for each charge pair that flipped stability, namely, lysine—aspartate, lysine—glutamate, and arginine—aspartate salt bridges. Figure 4a is a ridge plot of the charge pairs' inter-residue distance of each leading to middle and middle to trailing monomers. Each cationic containing lysine was measured from the N ζ amine to the anionic aspartates' C δ of the carboxyl group. The leading to middle (L to M) peptides for both the canonical OGDK and reverse OGKD had a population density within 5 Å. However, the more stabilizing DK reverse lateral interaction has a closer interaction population than that of the canonical KD lateral interaction. A representative rendering of each of the main, stabilizing conformers from the simulation is shown in Figure 4b.

Similar distance analyses of the lysine-glutamate (OGKE/OGEK), arginine-glutamate (OGRE/OGER), and arginine-aspartate (OGRD/OGDR) lateral substitutions are presented in the Supporting Information (Figures S19–S21). These MD

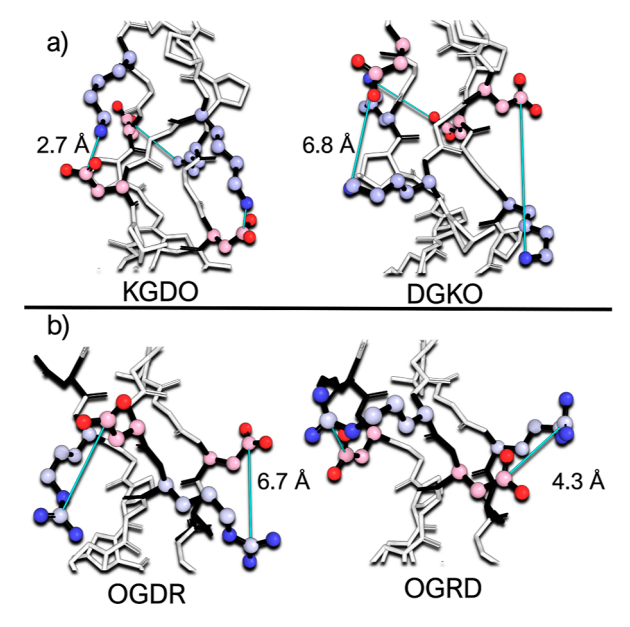


Figure 3. Packed models of charge pairs in triple helices. (a) KGDO substitutions yield two KD axial interactions and one lateral interaction; the axial interaction is in close proximity. The reverse sequence of the amino acids into DGKO shows an increased interaction distance and a less effective pairwise interaction. (b) OGDR substitutions yield two less favorable DR lateral interactions. For the lateral geometry, the reversing of the sequence into OGRD results in a closer interaction and is more stabilizing.

studies showed that the strongest supramolecular interaction in the peptide KGDO is able to have two axial interactions and one lateral interaction, all reaching within 3 Å. In Figure S20, the reverse D—R lateral charge distance is smaller than the R—D canonical interaction, with a maximum population density of 3.7 Å.

The Ramachandran plots for each interaction were used to quantify the ϕ - ψ angles about each substituted anion and

Interaction Distance of Reverse and Canonical Charge Pairs

Figure 4. MD of the lateral salt bridges interaction propensity. (a) A ridge plot compares the population density for each leading to the middle strand's (L to M) and middle to trailing strand's (M to T) interaction distance for a simulated OGKD (canonical, label 2) and OGDK (reverse, label 1) charge pair. OGKD has a larger population density within the 5 Å cutoff for positive, supramolecular interactions and closer to 3.3 Å maximum. (b) Snapshots from the MD trajectories that visualize the major, positive interactions for both the canonical and reverse charge pairs.

cation (Figures S22–S24) but qualitatively showed little difference. We conclude that differences in charge pair stability are primarily driven by their ability to be in close proximity.

Enhanced Stability with Covalent Capture. Previous work with covalent capture demonstrated not only the utility of providing extra stability and specificity to the triple helix but also biological applications, orthogonal synthetic schemes, and mechanistic elucidation. ^{24–26,34,35} Here we extended our investigation of the scope of covalent capture to include reverse, noncanonical charge pairs between lysine and either glutamate or aspartate. The four supramolecular peptides that were characterized above in Table 1 were also prepared for covalent capture and are summarized in Table 3.

Table 3. Enhanced Stabilization with a Covalent Capture

	supra. $T_{\rm m}$ (°C)	Cov. $T_{\rm m}$ (°C)	ΔT_{m}			
YGXO Substitutions						
KGEO ^a	43.5	60.5	+17.0			
EGKO	35.0	78.5	+43.5			
KGDO ^a	45.5	67.0	+19.5			
DGKO	32.5	dimer ^b				
OGXY Substitutions						
OGKE	36.0	60.0	+24.0			
OGKD	37.5	dimer ^b				

 $^aT_{\mathrm{m}}$ values from ref 25. b Unsuccessful trimerization, only a single isopeptide bond was observed.

The covalent capture experiments were conducted according to our previous method using mild coupling reagents EDC and HOBt. In the case of OGKE, ESI-MS (electrospray ionization-mass spectrometry) of the covalently captured triple helices corresponds to two water losses, indicating the formation of the covalently captured trimer from two EK lateral reverse salt bridges (Figure 5d). While a trimer should be covalently captured, only two amide bonds are expected because trailing to leading K–E amino acid distances are too far from one another. CD melting and refolding results of the supra-

molecular and covalently captured triple helices demonstrate a melting temperature of the supramolecular OGKE triple helix of 36 $^{\circ}$ C. Cooling from 85 to 5 $^{\circ}$ C with a rate of 10 $^{\circ}$ C/h, supramolecular OGKE triple helices only partially reform. For supramolecular triple helices, this hysteresis is often observed and indicates a slow assembly.

Similar melting and refolding experiments were conducted with the covalently captured OGKE triple helix (Figure 5f). With two amide covalent bonds connecting the three peptides, the melting temperature of the ccOGKE trimer is 60 °C, an increase of 24 °C. Compared to the covalent captured system with two axial and one lateral isopeptide bonds formed between the canonical K–E salt bridges which increased in thermal stability by 17 °C, this reverse charge pair covalently captured system is significantly more stabilized. Additionally, the refolding curve of the ccOGKE trimer is almost superimposed on the melting curve, indicating a significantly improved refolding rate. Despite the formation of fewer covalent bonds, our covalent capture experiments demonstrate that the reverse lateral salt bridge formed by EK interactions is a viable strategy to make stable collagen mimetic structures.

Covalent capture experiments were performed on EK reverse axial salt bridges using EGKO peptides (Figure 6b,c). The EGKO peptides were self-assembled into stable supramolecular triple helices with a melting temperature of 35 °C. After the covalent capture reaction, three isopeptide amide bonds were observed by MS to have formed (Figure 6d). The melting temperature of the covalently captured EGKO triple helix increased to 78.5 °C, which is 43.5 °C more stable than the supramolecular counterpart (Figure 6e,f). This is the highest stability gain among similar covalent captured systems we have ever observed. The refolding curve of the supramolecular EGKO triple helix shows increased MRE values as the temperature drops but a hysteresis is observed, indicating slow refolding kinetics. However, the covalently captured EGKO triple helix shows a perfectly overlaid refolding curve, suggesting that its folding kinetics are enhanced. Successful covalent capture further expands the utility of the charge pair

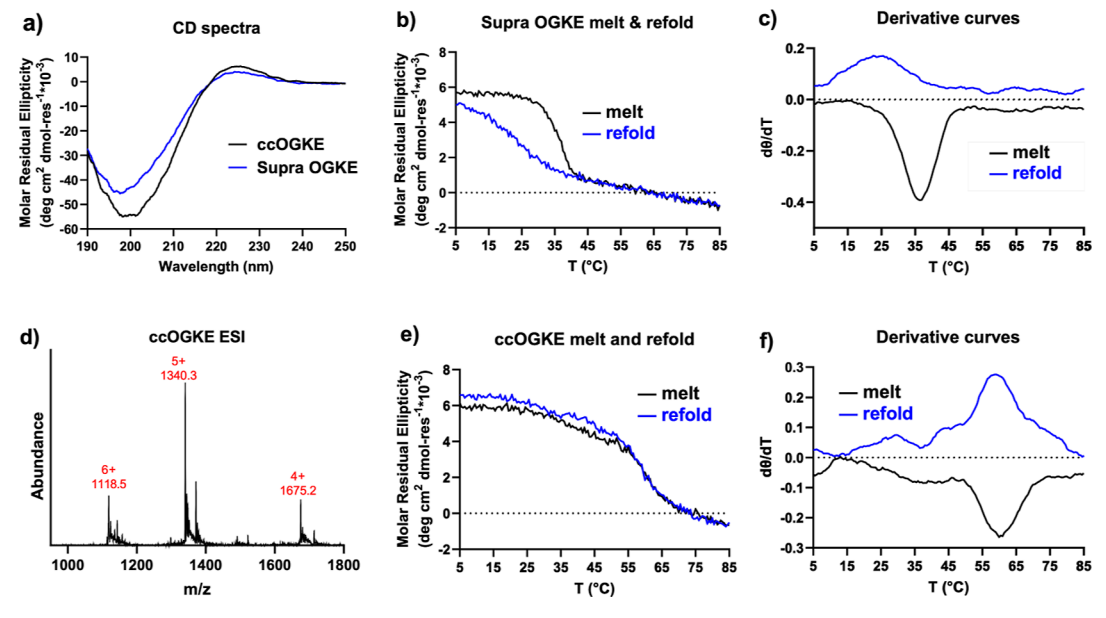


Figure 5. Covalent capture of the OGKE triple helices. (a) CD spectra of the supramolecular and covalently captured OGKE trimers, (b) CD melting and refolding curves of the supramolecular OGKE triple helix monitored at 225 nm, (c) derivative curves of the melting and refolding results in b, (d) ESI mass spectrometry of the covalently captured OGKE triple helix, (e) CD melting and refolding curves of the covalently captured OGKE triple helix, and (f) derivative curves of the melting and refolding curves in e.

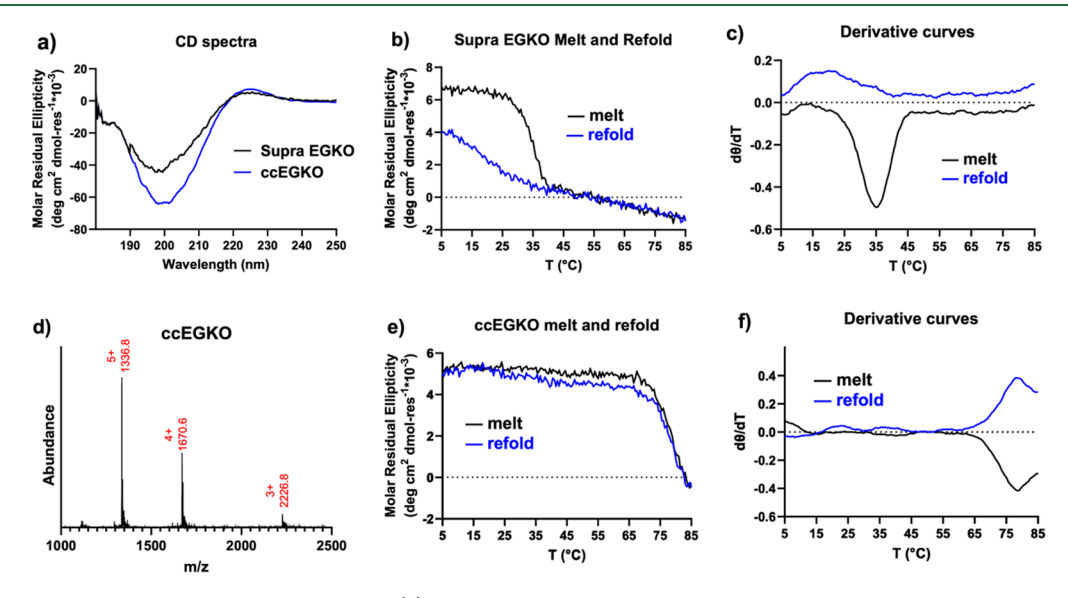


Figure 6. Covalent capture of the EGKO triple helices. (a) CD spectra of the supramolecular and covalently captured EGKO trimers, (b) CD melting and refolding curves of the supramolecular EGKO triple helix, (c) derivative curves of the melting and refolding results in b, (d) ESI mass spectrometry of the covalently captured EGKO triple helix, (e) CD melting and refolding curves of the covalently captured EGKO triple helix, and (f) derivative curves of the melting and refolding curves in e.

in engineering collagen mimetics. In particular, having an OGKE sequence is easier to incorporate in de novo design schemes, because the charge pair is contained in a single Xaa—Yaa—Gly triplet repeat.

Covalent capture of aspartate-containing peptides for axial and lateral reverse charge pairs was also attempted. These systems were inefficient, as we observed a single isopeptide bond and peptide dimer (Figures S14–S16). A complete summary of the covalently captured peptides is presented in Table 3.

Considerations for reverse salt bridges and their utility in de novo design have been exhaustively explored. Among the eight reverse charge pairs, both reverse, lateral DR and reverse, lateral DK interactions result in significant stabilization. However, only the DK lateral interaction appears strong enough to overcome destabilization from the inherent single amino acid propensity. We have also demonstrated that covalent hyperstabilization can occur for the reverse salt bridge of both axial and lateral KE interactions. These could be used to help stabilize particularly low thermal stability assemblies and further expand their scope in understanding biological processes.

CONCLUSIONS

Salt bridges are a crucial component of triple helix stabilization in both natural and synthetic systems. Expanding the scope of

usable pairwise interactions is crucial to recapitulate all of the beneficial structural components of natural collagen. Here, the use of supramolecular and covalently captured reverse charge pairs demonstrates new tools for enhancing the stability and specificity of collagens. Eight salt-bridge pairwise interactions were investigated from the supramolecular and covalently captured assemblies using both MD simulations and experimental techniques. DK reverse lateral interactions were found to be particularly effective in the supramolecular case. Covalent capture was observed to be successful, and enhanced thermal stability of the ccEGKO and ccOGKE peptides yielded a powerful tool for design. These supramolecular and covalent strategies are anticipated to be important in future synthetic collagen materials and applications.

ASSOCIATED CONTENT

Supporting Information

The Supporting Information is available free of charge at https://pubs.acs.org/doi/10.1021/acs.biomac.3c00680.

Full peptide characterization including UPLC, mass spectrometer data, CD melt curves; MD simulations; and further covalent capture characterization data (PDF)

AUTHOR INFORMATION

Corresponding Author

Jeffrey D. Hartgerink — Department of Chemistry, Rice University, Houston, Texas 77005, United States; Department of Bioengineering, Rice University, Houston, Texas 77005, United States; orcid.org/0000-0002-3186-5395; Phone: +1-713-348-2101; Email: jdh@rice.edu

Authors

Carson C. Cole — Department of Chemistry, Rice University, Houston, Texas 77005, United States; ⊚ orcid.org/0000-0002-7573-1882

Le Tracy Yu — Department of Chemistry, Rice University, Houston, Texas 77005, United States; orcid.org/0000-0001-9904-6460

Mikita Misiura – Department of Chemistry, Rice University, Houston, Texas 77005, United States

Joseph Williams, III – Department of Chemistry, Rice University, Houston, Texas 77005, United States

Thi H. Bui – Department of Chemistry, Rice University, Houston, Texas 77005, United States

Complete contact information is available at: https://pubs.acs.org/10.1021/acs.biomac.3c00680

Author Contributions

Carson C. Cole: conceptualization, methodology, investigation, writing. Le T. Yu: methodology, investigation, writing. Mikita Misiura: investigation, methodology. Joseph Williams III: conceptualization, data curation. Thi H. Bui: investigation, data curation. Jeffrey D. Hartgerink: editing, writing, supervision, funding acquisition.

Notes

The authors declare no competing financial interest.

ACKNOWLEDGMENTS

This work was funded in part by the National Science Foundation (CHE 2203937), the National Science Foundation Graduate Research Fellowship (grant no. 1842494), and the

Welch Foundation (C-2141). This work was also supported in part by the Big-Data Private-Cloud Research Cyberinfrastructure MRI award funded by the NSF under grant CNS-1338099 and by Rice University's Center for Research Computing (CRC).

REFERENCES

- (1) Hendsch, Z. S.; Tidor, B. Do salt bridges stabilize proteins? A continuum electrostatic analysis. *Protein Sci.* **1994**, *3*, 211–226.
- (2) Zhou, H.-X.; Pang, X. Electrostatic interactions in protein structure, folding, binding, and condensation. *Chem. Rev.* **2018**, *118*, 1691–1741.
- (3) Shoulders, M. D.; Raines, R. T. Collagen Structure and Stability. *Annu. Rev. Biochem.* **2009**, *78*, 929–958.
- (4) Brodsky, B.; Persikov, A. V. Fibrous Proteins: Coiled-Coils, Collagen and Elastomers; Advances in Protein Chemistry; Academic Press, 2005; Vol. 70, pp 301–339.
- (5) Gordon, M. K.; Hahn, R. A. Collagens. Cell Tissue Res. 2010, 339, 247-257.
- (6) Li, M. H.; Fan, P.; Brodsky, B.; Baum, J. Two-dimensional NMR assignments and conformation of (Pro-Hyp-Gly)10 and a designed collagen triple-helical peptide. *Biochemistry* **1993**, 32, 7377–7387.
- (7) Gauba, V.; Hartgerink, J. D. Self-Assembled Heterotrimeric Collagen Triple Helices Directed through Electrostatic Interactions. *J. Am. Chem. Soc.* **2007**, *129*, 2683–2690.
- (8) Fratzl, P.; Weinkamer, R. Nature's hierarchical materials. *Prog. Mater. Sci.* **2007**, *52*, 1263–1334.
- (9) Zhang, Y.; Herling, M.; Chenoweth, D. M. General solution for stabilizing triple helical collagen. *J. Am. Chem. Soc.* **2016**, *138*, 9751–9754
- (10) Bhowmick, M.; Fields, G. B. In *Peptide Modifications to Increase Metabolic Stability and Activity*; Cudic, P., Ed.; Humana Press: Totowa, NJ, 2013; pp 167–194.
- (11) Erdmann, R. S.; Wennemers, H. Functionalizable collagen model peptides. J. Am. Chem. Soc. 2010, 132, 13957–13959.
- (12) Kotch, F. W.; Raines, R. T. Self-assembly of synthetic collagen triple helices. *Proc. Natl. Acad. Sci. U.S.A.* **2006**, *103*, 3028–3033.
- (13) Xu, F.; Zahid, S.; Silva, T.; Nanda, V. Computational design of a collagen A: B: C-type heterotrimer. *J. Am. Chem. Soc.* **2011**, *133*, 15260–15263.
- (14) Fallas, J. A.; Lee, M. A.; Jalan, A. A.; Hartgerink, J. D. Rational Design of Single-Composition ABC Collagen Heterotrimers. *J. Am. Chem. Soc.* **2012**, *134*, 1430–1433.
- (15) Walker, D. R.; Hulgan, S. A. H.; Peterson, C. M.; Li, I.-C.; Gonzalez, K. J.; Hartgerink, J. D. Predicting the stability of homotrimeric and heterotrimeric collagen helices. *Nat. Chem.* **2021**, 13, 260–269.
- (16) Hentzen, N. B.; Islami, V.; Köhler, M.; Zenobi, R.; Wennemers, H. A Lateral Salt Bridge for the Specific Assembly of an ABC-Type Collagen Heterotrimer. *J. Am. Chem. Soc.* **2020**, *142*, 2208–2212.
- (17) Brodsky, B.; Ramshaw, J. A. M. The collagen triple-helix structure. *Matrix Biol.* **1997**, *15*, 545–554.
- (18) Persikov, A. V.; Ramshaw, J. A. M.; Brodsky, B. Prediction of collagen stability from amino acid sequence. *J. Biol. Chem.* **2005**, *280*, 19343–19349.
- (19) Cole, C. C.; Misiura, M.; Hulgan, S. A.; Peterson, C. M.; Williams, J. W.; Kolomeisky, A. B.; Hartgerink, J. D. Cation- π Interactions and Their Role in Assembling Collagen Triple Helices. *Biomacromolecules* **2022**, 23, 4645–4654.
- (20) Chiang, C.-H.; Fu, Y.-H.; Horng, J.-C. Formation of AAB-Type Collagen Heterotrimers from Designed Cationic and Aromatic Collagen-Mimetic Peptides: Evaluation of the C-Terminal Cation Interactions. *Biomacromolecules* **2017**, *18*, 985–993.
- (21) Persikov, A. V.; Ramshaw, J. A. M.; Kirkpatrick, A.; Brodsky, B. Amino Acid Propensities for the Collagen Triple-Helix. *Biochemistry* **2000**, *39*, 14960–14967.
- (22) Hennet, T. Collagen glycosylation. Curr. Opin. Struct. Biol. 2019, 56, 131–138.

- (23) Sun, T.; Qiang, S.; Lu, C.; Xu, F. Composition-dependent energetic contribution of complex salt bridges to collagen stability. *Biophys. J.* **2021**, *120*, 3429–3436.
- (24) Peterson, C. M.; Helterbrand, M. R.; Hartgerink, J. D. Covalent capture of a collagen mimetic peptide with an integrin-binding motif. *Biomacromolecules* **2022**, 23, 2396–2403.
- (25) Hulgan, S. A.; Jalan, A. A.; Li, I.-C.; Walker, D. R.; Miller, M. D.; Kosgei, A. J.; Xu, W.; Phillips, G. N., Jr.; Hartgerink, J. D. Covalent Capture of Collagen Triple Helices Using Lysine—Aspartate and Lysine—Glutamate Pairs. *Biomacromolecules* **2020**, *21*, 3772—3781.
- (26) Yu, L. T.; Hartgerink, J. D. Selective covalent capture of collagen triple helices with a minimal protecting group strategy. *Chem. Sci.* **2022**, *13*, 2789–2796.
- (27) Okuyama, K.; Miyama, K.; Mizuno, K.; Bächinger, H. P. Crystal structure of (Gly-Pro-Hyp)9: Implications for the collagen molecular model. *Biopolymers* **2012**, *97*, 607–616.
- (28) Maier, J. A.; Martinez, C.; Kasavajhala, K.; Wickstrom, L.; Hauser, K. E.; Simmerling, C. ff14SB: Improving the Accuracy of Protein Side Chain and Backbone Parameters from ff99SB. *J. Chem. Theory Comput.* **2015**, *11*, 3696–3713.
- (29) Abraham, M. J.; Murtola, T.; Schulz, R.; Páll, S.; Smith, J. C.; Hess, B.; Lindahl, E. GROMACS: High performance molecular simulations through multi-level parallelism from laptops to supercomputers. *SoftwareX* **2015**, *1*–2, 19–25.
- (30) Misiura, M.; Shroff, R.; Thyer, R.; Kolomeisky, A. B. DLPacker: deep learning for prediction of amino acid side chain conformations in proteins. *Proteins: Struct., Funct., Bioinf.* **2022**, *90*, 1278–1290.
- (31) Schrödinger, L.; DeLano, W. PyMOL. http://www.pymol.org/pymol (accessed Jan 22, 2023).
- (32) Horovitz, A.; Serrano, L.; Avron, B.; Bycroft, M.; Fersht, A. R. Strength and co-operativity of contributions of surface salt bridges to protein stability. *J. Mol. Biol.* **1990**, *216*, 1031–1044.
- (33) Debiec, K. T.; Gronenborn, A. M.; Chong, L. T. Evaluating the strength of salt bridges: a comparison of current biomolecular force fields. *J. Phys. Chem. B* **2014**, *118*, 6561–6569.
- (34) Li, I.-C.; Hulgan, S. A.; Walker, D. R.; Farndale, R. W.; Hartgerink, J. D.; Jalan, A. A. Covalent Capture of a Heterotrimeric Collagen Helix. *Org. Lett.* **2019**, *21*, 5480–5484.
- (35) Tanrikulu, I. C.; Raines, R. T. Optimal interstrand bridges for collagen-like biomaterials. *J. Am. Chem. Soc.* **2014**, *136*, 13490–13493.